



# Journal of Agrometeorology

ISSN : 0972-1665 (print), 2583-2980 (online)

Vol. No. 25 (4) : 510-516 (December - 2023)

<https://doi.org/10.54386/jam.v25i4.2286>

<https://journal.agrimetassociation.org/index.php/jam>



## Research Paper

### Comparative analysis of two parameter-dependent split window algorithms for the land surface temperature retrieval using MODIS TIR observations

JALPESH A. DAVE<sup>1\*</sup>, MEHUL R. PANDYA<sup>2</sup>, DHIRAJ B. SHAH<sup>3</sup>, HASMUKH K. VARCHAND<sup>1</sup>, PARTHKUMAR N. PARMAR<sup>1</sup>, HIMANSHU J. TRIVEDI<sup>1</sup>, VISHAL N. PATHAK<sup>3</sup>, MANOJ SINGH<sup>1</sup>, DISHA B. KARDANI<sup>3</sup>

<sup>1</sup>N. V. Patel College of Pure and Applied Sciences, CVM University, Vallabh Vidyanagar 388120, Gujarat, India

<sup>2</sup>Space Applications Centre, Indian Space Research Organisation, Ahmedabad 380015, Gujarat, India

<sup>3</sup>Sir P.T. Sarvajani College of Science, Veer Narmad South Gujarat University, Surat 395001, Gujarat, India

\*Corresponding Author: [davejalpesh1996@gmail.com](mailto:davejalpesh1996@gmail.com)

#### ABSTRACT

MODIS Land Surface Temperature (LST) product is extensively used in agricultural studies like crop health assessment, soil moisture estimation, irrigation management, land use land cover change, air-temperature retrieval and crop water stress detection. Numerous studies have used Split Window (SW) algorithm to retrieve LST from MODIS TIR bands. Among them, some utilize Sensor View Angle Dependent (SVAD) or Columnar Water Vapor Dependent (CWVD) SW algorithm. Present study aims to make use of SVAD and CWVD SW algorithms and compare them to evaluate the LST retrieval accuracy over various land surface type. Theoretical accuracy assessment of the CWVD and SVAD algorithms demonstrates a good accuracy with the an RMSE of 1.09K and 1.42K, respectively. The experimental retrieval of LST achieves exceptionally good accuracy, with a RMSE of 1.45K in the CWVD algorithm and 1.80K in the SVAD algorithm, particularly in heterogeneous regions. In homogeneous regions, the RMSE values are 1.14K in CWVD and 1.10K in SVAD. Both algorithms exhibit satisfactory accuracy; nevertheless, the application of these algorithms may vary in agricultural contexts. Based on the obtained results and the inclusion of required parameters, we have arrived at a conclusion regarding the superior performance of the SVAD compared to the CWVD for LST retrieval.

**Keywords:** Atmospheric radiative transfer equation, Land surface temperature, MODTRAN, MODIS, Split-Window

Land Surface Temperature (LST) as a fundamental parameter enables the identification of ideal land areas for target crop selection, while also serving various additional agronomical and meteorological purposes. These include crop pest and disease monitoring, water management optimization, plant stress assessment, yield estimation, weather forecasting, drought monitoring, climate change, surface energy balance, air-temperature and evapotranspiration retrieval (Heinemann *et al.*, 2020; Hu *et al.*, 2020; Fisher *et al.*, 2020; Li *et al.*, 2013; Shah *et al.*, 2012). The retrieved LST from satellite observations is ideal for water resource management, agricultural and meteorological studies because it provides frequent and extensive coverage data. In a recent study conducted by Parmar and Gontia (2019), LST was acquired from Landsat imagery, and they established the correlation between LST

and vegetation index, where they found that the LST decreases with an increase in the vegetation index. Retrieval of the LST using satellite data is an arduous and tactical process requiring information of a land cover type, sensor geometry, atmospheric parameters, and atmospheric transmittance. The Thermal InfraRed (TIR) region (8-14 $\mu$ m) is preferable for the LST retrieval, where only a few atmospheric constituents affect the radiation, mainly Water Vapor (WV) (Pandya *et al.*, 2011; Dave *et al.*, 2021). However, in the LST retrieval, the Land Surface Emissivity (LSE) has the most significant role because LSE overlaid atmospheric attenuation in the TIR region. The scientific community has dedicated many efforts to the implantation of methodology to retrieve LST from remotely sensed data. Some tremendously developed methods are Single Channel (SC) algorithm (Pandya *et al.*, 2014; Jiménez-Muñoz and

**Article info - DOI:** <https://doi.org/10.54386/jam.v25i4.2286>

Received: 26 July 2023; Accepted: 19 October 2023; Published online : 30 November, 2023

"This work is licensed under Creative Common Attribution-Non Commercial-ShareAlike 4.0 International (CC BY-NC-SA 4.0) © Author (s)"

Sobrino, 2009), hybrid Temperature Emissivity Separation (TES) algorithm (Gillespie *et al.*, 1998), Alpha derived emissivity method (Hulley *et al.*, 2021), Day-Night (D/N) measurement method (Li and Becker, 1993), Normalized Emissivity Method (NEM) (Valor *et al.*, 2003) and Multichannel algorithm also known as Split Window (SW) algorithm (Li *et al.*, 2013). Methods of retrieving LST employ various assumptions to account for the influence of atmospheric effect and LSE in the TIR region. Among them, SW algorithms are the most suitable method which utilizes two different adjacent absorption thermal bands for atmospheric correction and to differentiate the atmospheric properties (Price 1984). Prabhakara *et al.* (1974) discussed the basal knowledge of the SW algorithms to retrieve Sea Surface Temperature (SST) using Advanced Very High-Resolution Radiometer (AVHRR) data. Price (1984) took the lead in the LST SW technique; subsequently, Coll *et al.* (1994) enhanced the algorithm by adding spectral LSE and Sensor View Angle (SVA).

This study represents the intercomparison and sensitivity analysis of the Columnar Water Vapor (CWV)-Dependent (CWVD) and SVA-Dependent (SVAD) SW algorithms for the LST retrieval. SW coefficients have been derived for the Moderate Resolution Imaging Spectroradiometer (MODIS) TIR bands, and LST has been successfully retrieved using both SW algorithms over the Australian continent (Sobrino *et al.*, 1993). Here, SW coefficients have been derived through the utilization of simulated at-sensor radiance data generated by the MODerate resolution atmospheric TRANsmission (MODTRAN) 5.3 Radiative Transfer (RT) model. In this regard, 80235 at-sensor radiance simulations were computed using 80 SeeBor atmospheric profiles. The paper is structured as follows: it begins with study area and data used, then providing a detailed explanation of the atmospheric RT theory and theoretical background of the SW algorithm. Subsequently, the approach employed in this study is elaborated upon. The paper then proceeds to illustrate the discussion surrounding the derived SW coefficients, sensitivity analysis of the algorithms, and the accuracy assessment of the retrieved LST. Finally, the obtained outcomes from this study are presented in the conclusion, respectively.

## MATERIALS AND METHODS

### Study area and data used

In this study, cloud-free MODIS MYD09CMG and MYD11C1 data of the day 284 of 2020 has been acquired. There is no particular aim for the selection of data acquisition day. However, cloud-free data was the priority. The method has been applied in the Northern Territory, Southern, and Queensland of Australia. Australia has many different land covers, but most regions are covered by non-vegetate and open shrubland, and the second most land covers are cropland and forest (Sayre *et al.*, 2020). Therefore, this selected region is most suitable for the comparison of two different parameters-based on SW algorithm, as the larger homogeneity and heterogeneity of land cover provides steady results. Eighty SeeBor atmospheric profiles were utilized to simulate the at-sensor radiance. SeeBor database providing the global atmospheric profiles by comprising the satellite, laboratory and ground stations data (Borbas *et al.*, 2005). The profiles were carefully chosen within the range of  $0.1 \text{ gm} \cdot \text{cm}^{-2}$  to  $5.0 \text{ gm} \cdot \text{cm}^{-2}$ , apart from these are considered as saturated CWV.

### Fundamentals of atmospheric radiative transfer

At-sensor radiance is a vital parameter in satellite remote sensing, which is attenuated by atmospheric parameters. The phenomenon of atmospheric attenuation affecting a signal can be comprehensively elucidated by the RT theory, which can be expressed by the following equation.

$$L(T) = \varepsilon \cdot B(T_s) \cdot \tau + L^{\uparrow} + (1 - \varepsilon) \cdot L_{DWR}^{\downarrow} \cdot \tau \quad (1)$$

Where,  $L(T)$  represents the at-sensor radiance corresponding to a specific Brightness Temperature (BT) denoted as  $T$ ,  $B(T_s)$ , signifies Planck's radiation associated with the LST specified as  $T_s$ ,  $\tau$  is the atmospheric transmittance,  $L^{\uparrow}$  is the up-welling atmospheric radiance,  $L_{DWR}^{\downarrow}$  is the down-welling atmosphere radiance reflected from the surface to sensor and  $\varepsilon$  is the spectral LSE.

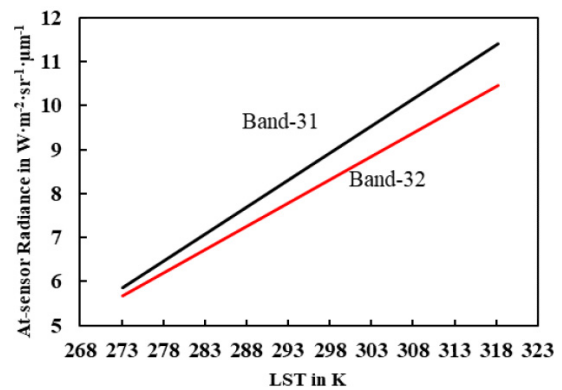


**Fig. 1:** Linear relation between radiance and LST for MODIS TIR Bands 31 & 32. The data has been obtained from the MODTRAN 5.3 RT model, employing a nadir view, with a land type of forest and a CWV value of  $3 \text{ gm} \cdot \text{cm}^{-2}$ .

The direct relation between at-sensor radiance and LST is clearly shown in the RT Equation (RTE). Accordingly, the direct and substantial contribution of the RTE becomes evident in the methods employed for the retrieval of LST. In most cases, a linear relationship exists between at-sensor radiance and LST. Fig. 1 shows the linear relation of the at-sensor radiance of MODIS TIR bands and LST for same land cover and atmospheric geometries, which are obtained using the MODTRAN 5.3 RT model-derived simulations. The disparity in both bands' at-sensor radiance is used for atmospheric correction in SW algorithms. Furthermore, this disparity varies with land cover types, atmospheric conditions and viewing geometries, which is resolved by utilizing a spectral LSE in the SW algorithm and also considering the effect of view angle.

### Theoretical perspective of split-window algorithm

The SW algorithm corrects the atmosphere effect using two adjacent atmospheric absorption bands and considering the minimal variation in the emissivity in the adjacent channels. It is applied for the LST retrieval by linear/non-linear annexation of at-sensor radiance or BT. Therefore, the SW method has been categorized into two parts, the linear SW method and the non-linear SW method. The general form of linear and non-linear SW

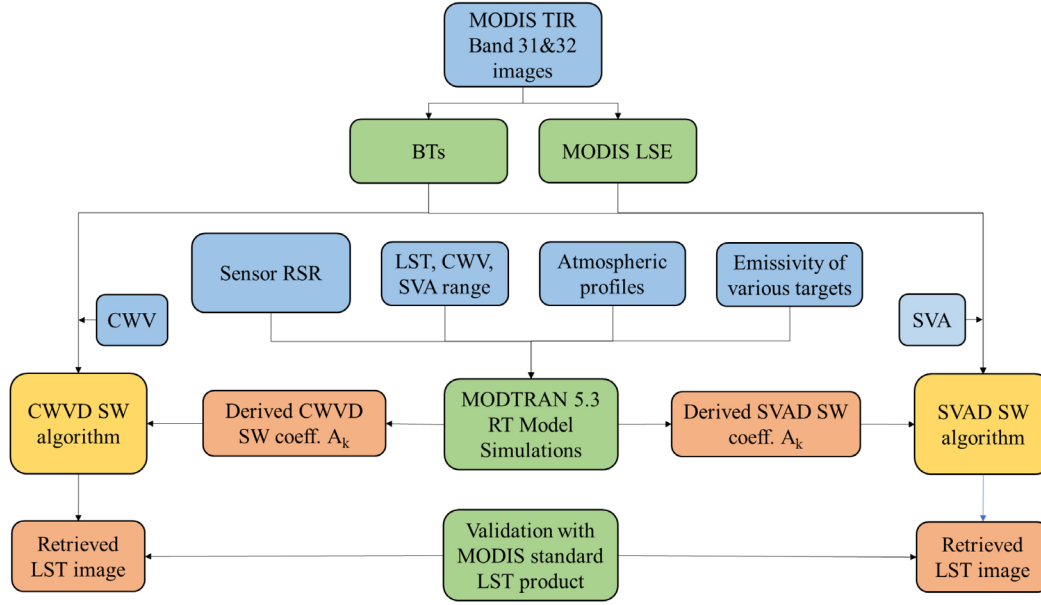


**Fig. 2:** Simple flow chart of SW algorithm development for LST retrieval using MODIS TIR data.

equations are as follows:

$$LST = A_0 + A_1 \cdot T_i + A_2 \cdot (T_i - T_j) \quad (2)$$

$$LST = A_0 + A_1 \cdot T_i + A_2 \cdot (T_i - T_j) + A_3 \cdot (T_i - T_j)^2 \quad (3)$$

Where,  $A_k$  are the SW coefficients,  $T_i$  and  $T_j$  are BT of bands  $i$  and  $j$ . The value of  $A_k$  ( $k = 0,1,2,3, \dots$ ) depends on spectral LSE, CWV, and SVA. Hence, numerous SW algorithms have been developed, wherein the dependent variables encompass combinations involving LSE, CWV, and SVA. In this study, the SW algorithm developed by Sobrino *et al.* (1993) has been used. It contained coefficients are least dependent on the atmosphere variability and highly dependent on LSE. Thus, the errors caused by LSE are easily evaluated, and the atmospheric changes are eliminated by developing different series of coefficients according to SVA or CWV. Therefore, the algorithm provides greater accuracy in highly volatile atmospheres and heterogenous land types. The analytical expression of the SW algorithm is.

$$T_s = A_0 + A_1 \cdot (T_i) + A_2 \cdot (T_i - T_j) + A_3 \cdot (T_i - T_j)^2 + A_4 \cdot (1 - \varepsilon) + A_5 \cdot d\varepsilon \quad (4)$$

Where  $T_s$  is LST,  $\varepsilon$  is the average LSE of the two bands ( $\varepsilon = (\varepsilon_i + \varepsilon_j)/2$ ), and  $d\varepsilon$  is the LSE difference of two bands ( $d\varepsilon = \varepsilon_i - \varepsilon_j$ ).

### The approach of split-window algorithms development

We have divided the present study into four parts; (1) Forward simulations of at-sensor radiance using MODTRAN 5.3 RT model; (2) Required inputs data collection and development of SW coefficients; (3) LST retrieval using MODIS TIR data; (4) Intercomparison of retrieved LST. By deriving significant inputs such as LSE and CWV from MODIS data, errors caused by these parameters are minimized in the algorithm. Total 80235 at-sensor

RT simulations were performed, encompassing variation in LST ranging from -10K to +15K in the step of 5K, CWV ranging from the  $0.1\text{gm}\cdot\text{cm}^{-2}$  to  $5.0\text{gm}\cdot\text{cm}^{-2}$  in the step of  $0.5\text{gm}\cdot\text{cm}^{-2}$ , and SVA: 0,10,20,30,35,40 and up to 70 degree. These simulations were conducted for various International Geosphere–Biosphere Programme (IGBP) land classes, including evergreen broadleaf forest, open and closed scrub, savanna, woody savanna, grassland, cropland, water and urban area. The spectral at-sensor radiances obtained from simulations using the MODTRAN 5.3 RT model have been converted into specific finite bands corresponding to the sensor's Relative Spectral Response (RSR) function. RSR of both TIR bands 31 and 32 of MODIS terra has been used. The weighted average value has been found using the following equation.

$$L_\lambda = \frac{\int l(\lambda) \cdot f(\lambda) \cdot d\lambda}{\int f(\lambda) \cdot d\lambda} \quad (5)$$

$L_\lambda$  is the weighted average value of at-sensor radiance,  $l(\lambda)$  is spectral at-sensor radiance, and  $f(\lambda)$  is the RSR of a specific band of MODIS. The obtained weighted at-sensor radiance for both bands converted into the BT ( $T_i$  and  $T_j$ ) using Planck's radiance equation. SW coefficients of both algorithms have been derived by applying linear statistical regression analysis over the SW equation (4). The coefficients are categorized into various ranges of CWV and SVA for a particular algorithm. The utilization of categorical coefficients provides a higher level of accuracy in estimating LST compared to employing a wide range of coefficients.

CWVD and SVAD SW algorithms have been formulated based on derived coefficients. The selection of categorized coefficients is based on the input values of CWV and SVA. Subsequently, LST is retrieved using pertinent parameters such as LSE and BT. The LST obtained through both techniques was compared against the standard LST product of MODIS to evaluate their accuracy. The analysis of results obtained from both SW algorithms revealed very good accuracy, and subsequently,

**Table 1:** Derived SW coefficients of CWVD.

CWV in $\text{gm}\cdot\text{cm}^{-2}$	$A_0$	$A_1$	$A_2$	$A_3$	$A_4$	$A_5$	$R^2$	Standard Error in K
[0.10,0.25]	-10.0701	1.0336	-1.5589	0.1275	79.5348	70.6006	0.9995	0.21
[0.25,1.00]	-12.6088	1.0426	-1.5856	0.0786	77.7766	69.9523	0.9992	0.27
[1.00,2.50]	-31.0442	1.1104	-1.0864	0.2317	56.5995	26.5681	0.9882	1.09
[2.50,3.70]	-47.8013	1.1763	6.8228	-0.5516	34.8731	-159.732	0.9565	1.95
[3.70,5.00]	01.8715	0.9986	9.7931	-0.0752	28.9096	-85.8281	0.8865	2.46

**Table 2:** Derived SW coefficients of SVAD.

SVA in Degree	$A_0$	$A_1$	$A_2$	$A_3$	$A_4$	$A_5$	$R^2$	Standard Error in K
[00.00,20.00]	-20.0436	1.0750	4.1566	1.1340	33.3528	-258.1199	0.9798	1.41
[20.00,27.50]	-21.0130	1.0787	4.1249	1.3011	33.0241	-257.1598	0.9789	1.44
[27.50,32.50]	-22.3506	1.0839	4.1068	1.4758	32.7158	-255.1758	0.9776	1.49
[32.50,37.50]	-23.3244	1.0876	4.1124	1.5696	32.5541	-253.6251	0.9766	1.52
[37.50,42.50]	-24.5585	1.0923	4.1390	1.6591	32.3861	-251.7027	0.9754	1.56
[42.50,47.50]	-26.1102	1.0983	4.1997	1.7377	32.1928	-249.5261	0.9736	1.62
[47.50,52.50]	-28.1320	1.1061	4.3118	1.8051	31.9380	-247.2287	0.9712	1.69
[52.50,57.50]	-30.7948	1.1165	4.5036	1.8613	31.5466	-245.1428	0.9677	1.79
[57.50,62.50]	-34.4207	1.1307	4.8151	1.9189	30.9026	-243.3981	0.9623	1.93
[62.50,67.50]	-39.6981	1.1518	5.3370	2.0022	29.8265	-241.9671	0.9532	2.15
[67.50,72.50]	-48.0154	1.1858	6.3038	2.1728	27.9547	-239.9701	0.9353	2.54

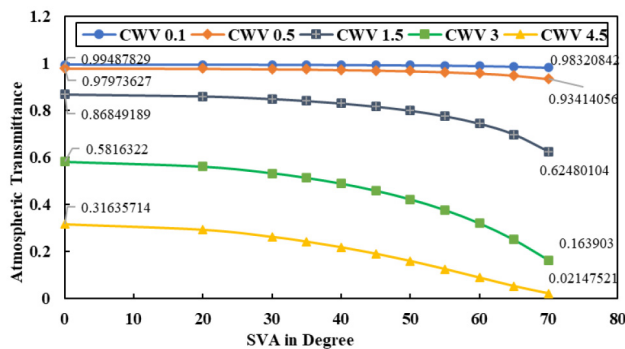


**Fig. 3:** Atmospheric transmittance is the function of the SVA for various CWV values, data have been derived from the MODTRAN 5.3 RT model for the tropical atmosphere at a 300K LST.

a comparative assessment between these two algorithms was conducted. Under the development of this study, the following steps were carried out and shown in the flow chart (Fig. 2).

**RESULTS AND DISCUSSION**

*Analysis of obtained split-window coefficients*

CWVD and SVAD SW algorithms have been developed for the LST retrieval and investigated the accuracy of both algorithms. The SW algorithm contains six coefficients that depend independently on surface and atmospheric parameters. The coefficients of CWVD algorithm are defined for five distinct ranges of CWV. Table 1 displays the coefficients, standard error and  $R^2$  values for each respective range. Here, the maximum standard error of the theoretical algorithm is 2.46K at a higher value of CWV.

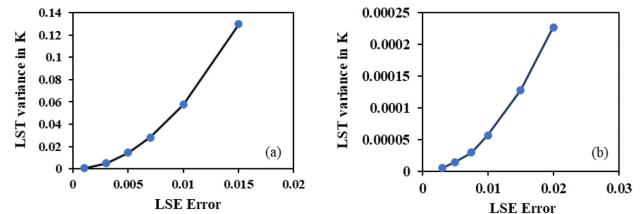


**Fig. 4:** LST error in K for different LSE errors. (a) CWVD SW algorithm; (b) SVAD SW algorithm.

The error exhibits an increasing trend as CWV values range from lower to higher values, primarily attributed to the variability of atmospheric transmission.

An analysis of atmospheric transmittance is conducted across specific MODIS TIR band, considering different values of CWV. As the CWV increases, the atmospheric transmittance decreases, at the higher values of CWV, the combined effects of CWV and SVA are responsible for significant decrement (Fig. 3). In Fig. 3, the transmittance decreases from 0.3163 to 0.0214 as SVA increases from smaller to larger values, particularly at higher CWV value ( $4.5\text{gm}\cdot\text{cm}^{-2}$ ).

In Fig. 3, there is no significant change in transmittance up to 20 degrees. Therefore, we developed a single coefficient for the SVA range from 0 to 20 degree, then, coefficients are developed in the interval of 5 degrees ranges from 20 to 72 degrees as significant changes are observed at higher values of SVA. The developed SVAD SW coefficients have been alienated into eleven ranges of SVA (Table 2). The standard error and  $R^2$  values demonstrate a high level of accuracy for SVAD algorithm. The standard error remains below

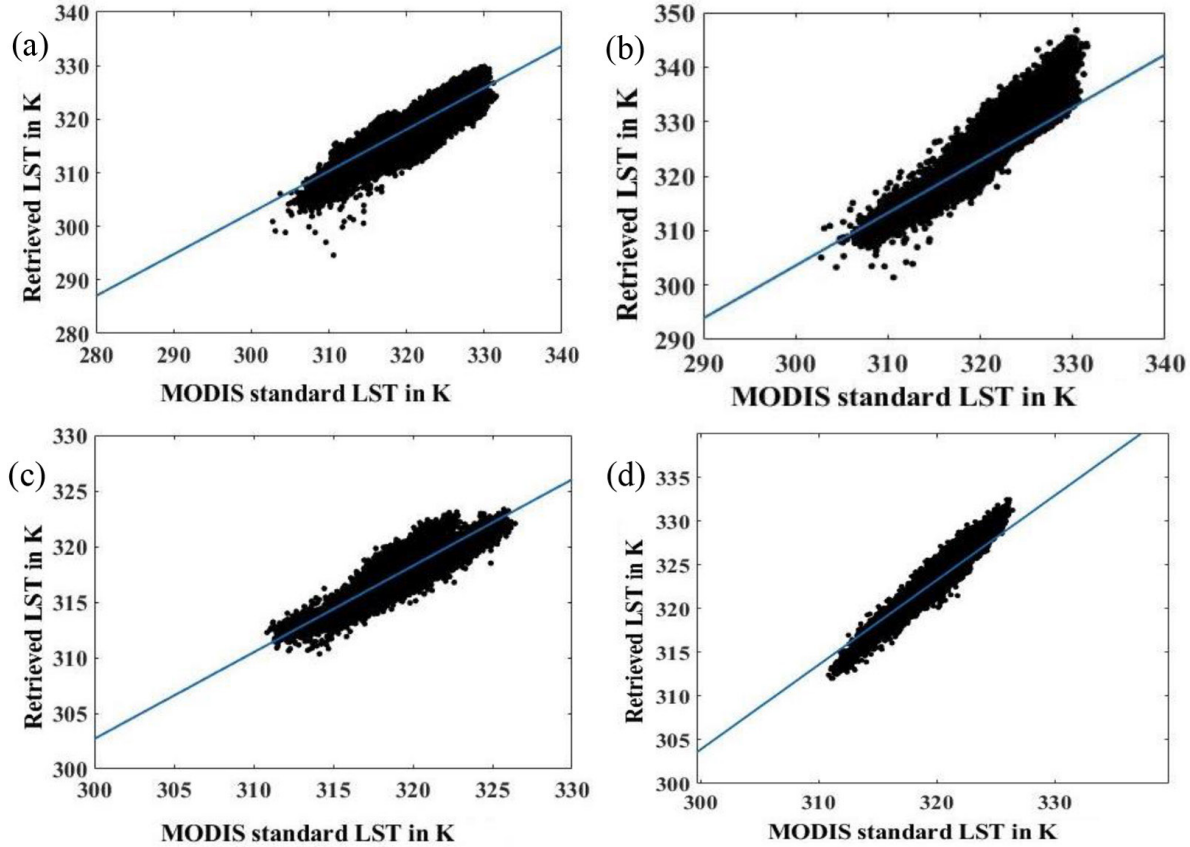


**Fig. 5:** Comparison between MODIS LST and retrieved LST in K. (a) For the CWVD SW algorithm, land type: Heterogeneous; (b) For the SVAD SW algorithm, land type: Heterogeneous; (c) For the CWVD SW algorithm, land type: Homogeneous; (d) For the SVAD SW algorithm, land type: Homogeneous.

2.54K up to 72.50 degrees, indicating the successful development of the algorithm and coefficients.

#### Sensitivity analysis of developed split-window algorithms

The development of the SW algorithm for retrieving LST requires LSE, CWV, SVA and at-sensor BT. Therefore, errors in those parameters can affect the accuracy of LST. In the present study, nine various LSE have been taken during the algorithm development. The SW algorithm (Sobrino *et al.*, 1993) is highly sensitive and dependent on LSE and least sensitive to the atmospheric WV as discussed earlier. Therefore, the LSE error's impact on LST must be studied in the development of the algorithm. The following equation has been used to analyse the LSE error on the SW algorithm for retrieving LST.

$$\delta T_s = |T_s(x + \delta x) - T_s(x)| \quad (6)$$

Where  $\delta T_s$  is the LST error,  $x$  is LSE, and  $\delta x$  is considered the LSE error,  $T_s(x + \delta x)$  and  $T_s(x)$  are retrieved LST with the value of  $(x + \delta x)$  and  $(x)$ , respectively. The sensitivity analysis was carried out over eighty thousand simulations datasets and calculated Root Mean Square Error (RMSE) of bias and standard deviation. This analysis has been carried out for both SW algorithms (Fig. 4).

The sensitivity analysis was carried out for the each values of SVA and CWV. Analysis has been done using the Analysis

of Variance (ANOVA) single-factor test. The LST error variance of various CWV or SVA has been derived for particular LSE error. For example, when considering an LSE error of 0.015, the LST error variance indicates how much the average LST error increases with an increase in CWV or SVA. A higher variance signifies a greater influence of the LSE error on the LST error. The LST error variance in the CWVD algorithm is 0.0005K, 0.0051K, 0.0144K, 0.0282K, 0.0566K, 0.0576K, 0.1297K, for 0.001, 0.003, 0.005, 0.007, 0.01, 0.015 LSE error (Fig. 4a). The LST error variance in the SVAD algorithm is 5.10094E-06K, 1.41803E-05K, 2.92396E-05K, 5.67451E-05K, 0.00012767K, 0.000226975K for 0.003, 0.005, 0.0075, 0.01, 0.015, 0.02 LSE error (Fig. 4b).

#### Accuracy assessment of retrieved LST

Developed SVAD and CWVD SW algorithms have been applied over two different land types (Homogeneous and Heterogeneous) on MODIS TIR data for the LST retrieval. The proper land types selection has been performed using the MODIS world land use and land cover data. Accuracy assessment of the retrieved LST is the most essential for understanding accuracy of the algorithms. Here, we used MODIS standard LST data products as reference for the assessment. Pixel-to-pixel comparisons between MODIS LST and retrieved LST have been represented by a scatter graph (Fig. 5). In the previous section, we discussed the variability of LSE, making retrieving LST more challenging. Therefore, we

applied both algorithms on the heterogeneous and homogeneous land types to check the accuracy of the developed algorithms. The pixel-to-pixel comparison of retrieved and standard MODIS LST images has been carried out; each black dot in the scatter graph represents the pixel values of LST images.

Fig. 5 (a) and (b) represent the heterogeneous land type, whereas (c) and (d) for the homogeneous land type. The R<sup>2</sup> value for all four conditions is 0.99, which shows the good correlations between the retrieved LST and MODIS LST. Nevertheless, the RMSE for the heterogeneous land type is 1.45K in the CWVD algorithm and 1.80K in the SVAD SW algorithm (Fig. 5 (a) and (b)), while for the homogeneous land type, it is 1.14K in CWVD and 1.10K in SVAD SW algorithm (Fig. 5 (c) and (d)).

### CONCLUSION

This study evaluates the accuracy of SW algorithms based on SVA and CWV to determine the most reliable and accurate approach for the LST retrieval. The SVAD and CWVD algorithms derived LST pixel values are outstandingly matching with MODIS LST over different land covers and various values of CWV and SVA. A comparison of the retrieved LST results of both algorithms with MODIS LST shows R<sup>2</sup> values of 0.99 with an RMSE range from 1.10K to 1.80K. According to the result, the SVAD SW algorithm is more reliable than the CWVD SW algorithm as most of the satellites provide SVA, which makes LST retrieval easy. In contrast, the CWVD SW algorithm requires CWV values at the time of satellite over pass. Therefore, the value of CWV has to be obtained either from the ground station or using the direct product of CWV, which construct the method prolonged and also affects the accuracy. Therefore, SVAD algorithm will be highly reliable in agricultural applications. For instance, plant stress assessment and evapotranspiration requires geometric arrangements of the crop, which impacts in leaf area index and canopy architecture. However, in the development of the SVAD algorithm, the prior knowledge of atmospheric effect on the signal is must for the optimum algorithm accuracy.

### ACKNOWLEDGEMENT

The authors express their gratitude to Dr Basudeb Bakshi, Principal of N. V. Patel College of Pure and Applied Sciences, Vallabh Vidyanagar, and Shree Nilesh M. Desai, Director of SAC-ISRO, Ahmedabad, for their inspiration and support throughout this study. Additionally, we acknowledge the LAADS DAAC for providing the MODIS data.

**Conflict of interest:** The authors declare that there is no conflict of interest related to this article.

**Funding:** This research was undertaken independently without any external financial support.

**Data availability:** Data to be provided on request.

**Author contribution:** **J. A. Dave:** Writing-original draft preparation, At-sensor radiance simulations, Algorithm development, Implementation, and Result analysis. **M. R. Pandya:** Conceptualisation, Writing-original draft preparation, Formal

analysis, Resources, Providing necessary qualitative and quantitative inputs. **D. B. Shah:** Important suggestions, Deliberations during simulations, and Writing of the manuscript. **H. K. Varchand:** Original draft preparation, At-sensor radiance simulations and Data curation. **P. N. Parmar:** Original draft preparation, At-sensor radiance simulations and Data curation. **H. J. Trivedi:** Original draft preparation, Conceptualisation and facilitating the work. **V. N. Pathak:** Important suggestions, Deliberations during simulations, and Writing of the manuscript. **M. Singh:** Important suggestions, Deliberations during simulations, and Writing of the manuscript. **D. B. Kardani:** Important suggestions, Deliberations during simulations, and Writing of the manuscript.

**Disclaimer:** The contents, opinions, and views expressed in the research article published in the Journal of Agrometeorology are the views of the authors and do not necessarily reflect the views of the organizations they belong to.

**Publisher's Note:** The periodical remains neutral with regard to jurisdictional claims in published maps and institutional affiliations.

### REFERENCES

- Coll, C., Caselles, V., Sobrino, J. A. and Valor, E. (1994). On the atmospheric dependence of the split-window equation for land surface temperature. *Int. J. Remote Sens.*, 15(1), 105-122. <https://doi.org/10.1080/01431169408954054>
- Borbas, E., Seemann, S. W., Huang, H. L., Li, J. and Menzel, W. P. (2005). Global profile training database for satellite regression retrievals with estimates of skin temperature and emissivity. *In Proc. 14th Int. ATOVS Study Conf.*, 763-770. [http://cimss.ssec.wisc.edu/training\\_data/data/itsc14\\_borbas\\_trainingData.pdf](http://cimss.ssec.wisc.edu/training_data/data/itsc14_borbas_trainingData.pdf)
- Dave, J. A., Pandya, M. R., Pathak, V. N., Shah, D. B. and Trivedi, H. J. (2021). Development of View Angle Dependent Split-Window Algorithm for Retrieving Land Surface Temperature From Modis Thermal Infrared Data. *In 2021 IEEE International India Geoscience and Remote Sensing Symposium (InGARSS)*, 261-264. IEEE. <https://doi.org/10.1109/InGARSS51564.2021.9791897>
- Fisher, J. B., Lee, B., Purdy, A. J., Halverson, G. H., Dohlen, M. B., Cawse-Nicholson, K., ... and Hook, S. (2020). ECOSTRESS: NASA's next generation mission to measure evapotranspiration from the international space station. *Water Resour. Res.*, 56(4), e2019WR026058. <https://doi.org/10.1029/2019WR026058>
- Gillespie, A., Rokugawa, S., Matsunaga, T., Cothorn, J. S., Hook, S., & Kahle, A. B. (1998). A temperature and emissivity separation algorithm for Advanced Spaceborne Thermal Emission and Reflection Radiometer (ASTER) images. *IEEE Trans. Geosci. Remote Sens.*, 36(4), 1113-1126. <https://doi.org/10.1109/36.700995>
- Heinemann, S., Siegmann, B., Thonfeld, F., Muro, J., Jedmowski, C., Kemna, A., ... and Rascher, U. (2020). Land surface temperature retrieval for agricultural areas using a novel

- UAV platform equipped with a thermal infrared and multispectral sensor. *Remote Sens.*, 12(7), 1075. <https://doi.org/10.3390/rs12071075>
- Hu, T., Renzullo, L. J., van Dijk, A. I., He, J., Tian, S., Xu, Z., ... and Liu, Q. (2020). Monitoring agricultural drought in Australia using MTSAT-2 land surface temperature retrievals. *Remote Sens. Environ.*, 236, 111419. <https://doi.org/10.1016/j.rse.2019.111419>
- Hulley, G. C., Göttsche, F. M., Rivera, G., Hook, S. J., Freepartner, R. J., Martin, M. A., ... and Johnson, W. R. (2021). Validation and quality assessment of the ECOSTRESS level-2 land surface temperature and emissivity product. *IEEE Trans. Geosci. Remote Sens.*, 60, 1-23. <https://doi.org/10.1109/TGRS.2021.3079879>
- Jiménez-Muñoz, J. C., and Sobrino, J. A. (2009). A single-channel algorithm for land-surface temperature retrieval from ASTER data. *IEEE Geosci Remote Sens.*, 7(1), 176-179. <https://doi.org/10.1109/LGRS.2009.2029534>
- Li, Z. L. and Becker, F. (1993). Feasibility of land surface temperature and emissivity determination from AVHRR data. *Remote Sens. Environ.*, 43(1), 67-85. [https://doi.org/10.1016/0034-4257\(93\)90065-6](https://doi.org/10.1016/0034-4257(93)90065-6)
- Li, Z. L., Tang, B. H., Wu, H., Ren, H., Yan, G., Wan, Z., ... and Sobrino, J. A. (2013). Satellite-derived land surface temperature: Current status and perspectives. *Remote Sens. Environ.*, 131, 14-37. <https://doi.org/10.1016/j.rse.2012.12.008>
- Pandya, M. R., Shah, D. B., Trivedi, H. J. and Panigrahy, S. (2011). Simulation of at-sensor radiance over land for proposed thermal channels of Imager payload onboard INSAT-3D satellite using MODTRAN model. *J. Earth Syst. Sci.*, 120, 19-25. <https://doi.org/10.1007/s12040-011-0014-4>
- Pandya, M. R., Shah, D. B., Trivedi, H. J., Darji, N. P., Ramakrishnan, R., Panigrahy, S., ... and Kirankumar, A. S. (2014). Retrieval of land surface temperature from the Kalpana-1 VHRR data using a single-channel algorithm and its validation over western India. *ISPRS J. Photogramm Remote Sens.*, 94, 160-168. <https://doi.org/10.1016/j.isprsjprs.2014.05.004>
- Parmar, H. V. and Gontia, N. K. (2019). Derivation of land surface temperature using satellite imagery and its relationship with vegetation index. *J. Agrometeorol.*, 21(1), 104-106. <https://doi.org/10.54386/jam.v21i1.215>
- Prabhakara, C., Dalu, G. and Kunde, V. G. (1974). Estimation of sea surface temperature from remote sensing in the 11-to 13- $\mu$ m window region. *J. Geophys. Res.*, 79(33), 5039-5044. <https://doi.org/10.1029/JC079i033p05039>
- Price, J. C. (1984). Land surface temperature measurements from the split window channels of the NOAA 7 Advanced Very High Resolution Radiometer. *JGR Atmosph.*, 89(D5), 7231-7237. <https://doi.org/10.1029/JD089iD05p07231>
- Sayre, R., Karagulle, D., Frye, C., Boucher, T., Wolff, N. H., Breyer, S., ... & Possingham, H. (2020). An assessment of the representation of ecosystems in global protected areas using new maps of World Climate Regions and World Ecosystems. *Glob. Ecol. Conserv.*, 21, e00860. <https://doi.org/10.1016/j.gecco.2019.e00860>
- Shah, D. B., Pandya, M. R., Trivedi, H. J. and Jani, A. R. (2012). Estimation of minimum and maximum air temperature using MODIS data over Gujarat. *J. Agrometeorol.*, 14(2), 111-118. <https://doi.org/10.54386/jam.v14i2.1403>
- Sobrino, J. A., Caselles, V. and Coll, C. (1993). Theoretical split-window algorithms for determining the actual surface temperature. *Il Nuovo Cimento C*, 16, 219-236. <https://doi.org/10.1007/BF02524225>
- Valor, E., Coll, C., Caselles, V. and Niclos, R. (2003). The Adjusted Normalized Emissivity Method (ANEM) for land surface temperature and emissivity recovery. In IGARSS 2003. 2003 *IEEE International Geosci. Remote Sens. Symp.. Proceed.* (IEEE Cat. No. 03CH37477), 5, 3088-3090. IEEE. <https://doi.org/10.1109/IGARSS.2003.1294692>